
A NOVEL PHASE-NOISE MODULE FOR THE QUCS CIRCUIT SIMULATOR. PART I : THE PERIODIC STEADY-STATE.

arXiv PREPRINT

Torsten Djurhuus *

Goethe-University Frankfurt
t.djurhuus@physik.uni-frankfurt.de

Viktor Krozer

Goethe-University Frankfurt &
Ferdinand-Braun-Institut, Leibniz
Institut für Höchstfrequenztechnik
krozer@physik.uni-frankfurt.de

December 12, 2025

ABSTRACT

The paper discusses work done to expand and extend the capabilities of the open-source QUCS circuit simulator through the implementation of a computationally efficient time-domain steady-state analysis module, supporting simulation of autonomous circuits. To our knowledge, this represents the first time such an analysis module has been implemented in the QUCS environment. Hitherto, the only available option was a harmonic-balance module which was strictly limited to non-autonomous (driven) circuits. The research has several important scientific and industrial applications in the area of large-signal steady-state analysis of autonomous circuits *e.g.* free-running and coupled oscillator circuit networks. The reported results will have great impact *w.r.t.* analyzing, synthesizing and optimizing oscillatory behavior of various important industrial circuits and systems. The developed tool, furthermore, introduces support for simulating noise performance of circuits operating under large-signal conditions. This paper is the first part of a two-part series documenting the implementation of a novel (coupled)-oscillator phase-noise simulator engine in the QUCS environment. The goal of this undertaking is the advancement of the open-source QUCS project towards becoming a viable competitor to the commercial simulators currently on the market.

Keywords periodic steady-state, numerical analysis, circuit simulation, circuit analysis, autonomous circuits, oscillators, oscillator phase-noise.

1 Introduction

Efficient and rigorous modelling tools for analyzing, synthesizing and optimizing the large-signal Periodic Steady-State (PSS) of non-linear driven and autonomous circuits play a critical role in the design cycle of various circuits with important applications in *e.g.* modern communication and remote-sensing systems. Given the ever-increasing complexity of contemporary device models, and scale of modern circuit schematics, such work necessitates using an Electronic-Design-Automation (EDA) simulation program.

The work described herein considers the open-source Quite Universal Circuit Simulator (QUCS) [1,2], published under the GNU General Public License (GPL). The QUCS project was initiated in 2005 [1] and has since gone through several development cycles, updates and tests resulting in a robust and computationally efficient simulator for analysis of large-scale digital and analog circuits including an accessible Graphical User Interface (GUI) for schematic capture. The distribution comes with several important device models built-in and includes an interface for both the Verilog and VHDL hardware description languages. The QUCS distribution contains two main modules : the simulation engine, known as qucsator, and the GUI application for schematic capture. They communicate through a text-file based

*The authors are with the Institute of Physics, Goethe University of Frankfurt am Main, Max-von- Laue-Strasse 1, 60438, Frankfurt am Main. (correspondence e-mail: t.djurhuus@physik.uni-frankfurt.de).

netlist interface powered by a flex/yacc interpretation application. Herein, a choice was made to use the GUI application from the open-source (GPL) QUCS-S distribution [3–5] instead of the original QUCS GUI program. The QUCS-S distribution represents a QUCS clone project, inheriting various modules from the original package while also adding a new GUI application & external SPICE engine compatibility. It is furthermore able to directly interface with the original qucsator engine module. The package heritage structure described here was chosen after facing various practical problems installing the original QUCS GUI application on our workstation.

Unlike commercial counterparts, such as *e.g.* Keysight-ADS[®] or Cadence SpectreRF[®], the QUCS package currently has no option for steady-state analysis of autonomous circuits (*e.g.* free-running oscillators). A large-signal harmonic-balance (HB) simulator is included in the distribution, but this analysis option is limited to non-autonomous circuits *e.g.* driven RF power amplifiers. Autonomous circuits, such as free-running oscillators/clocks, injection-locked & phase-locked systems, bilaterally coupled oscillators *etc.*, represent critically important circuit modules in modern communication and remote-sensing systems. The design of these applications necessitate robust numerical analysis tools for proper circuit development and design. Specifically, a PSS simulation tool is fundamentally important in-order to estimate, analyze, synthesize and optimize autonomous circuits *w.r.t.* output signal power, steady-state frequency and stability of the large-signal solution. An option for simulating the PSS is furthermore required in-order to evaluate the large-signal noise-response [6–11] of (coupled) oscillator and clock circuit modules which are ubiquitous in modern electronic communication systems.

The QUCS/QUCS-S project clone, described here, is referred to as the QUCS-COPEN (working title) project/distribution/package *etc.* with the acronym COPEN standing for Coupled Oscillator Phase-Noise. The QUCS-COPEN project is currently a work-in-progress and, as the name suggest, involves the implementation of a phase-noise (PNOISE) analysis tool. This planned PNOISE engine module, which is based on a novel model developed by the authors in [11], requires a numerically calculated PSS solution and hence depend directly upon the engine API developed herein. The implementation of the QUCS-COPEN PNOISE module is discussed in part 2 of this paper-series.

1.1 A Note on Alternative Open-Source Engines : qucsatorRF, GnuCap, ngspice & Xyce.

The QUCS-S software package [3–5] ships with its own qucsator engine clone called qucsatorRF. From a quick initial inspection, this package looks very similar to the original. The qucsatorRF engine, being a clone of the qucsator engine, also does not contain a PSS module for autonomous circuit analysis (see qucsator discussion above). A choice was made to exclusively work with the original qucsator engine for the QUCS-COPEN project.

Both the QUCS and QUCS-S packages include the option to link to other non-QUCS, SPICE based, open-source engines. The QUCS suite includes an interface to the GnuCap package [12] whereas QUCS-S links to both the ngspice [13] and Xyce [14] engines. According to the latest published manual, the GnuCap API does not currently support any type of large-signal steady-state analysis [12]. The Xyce simulator does support PSS analysis of driven/non-autonomous circuits (similarly to the qucsator & qucsatorRF engines) but, importantly, does not support PSS analysis of autonomous circuits [14, section 7.7, second paragraph].

The latest ngspice manual release does indeed talk about a PSS option for autonomous circuits [13, section 11.3.12]. Importantly, this entry emphasizes (first line) : *"Experimental code, not yet made publicly available."* Very little information exists *w.r.t.* this PSS algorithm which, as far as the authors can tell, is only discussed in two sets of presentation slides [15, 16] and very briefly in the paper [17]. In the slides of [15, 16] the algorithm is referred to as the *transient shooting* (TRAN-SHOOT) method. Despite its name, this algorithm seems to have very little in common with the classical shooting method (PSS-SHOOT) [18–20]. The PSS-SHOOT algorithm, utilized herein (see discussion below in section 2), defines the PSS as the zero of non-linear system of equations. This represents a clearly stated problem with a well-understood solution procedure *i.e.* numerical multidimensional root finding. On the other hand, the lack of documentation, makes it very difficult to gauge the performance and convergence properties of the experimental TRAN-SHOOT method. From our perspective, several open questions exist *w.r.t.* the TRAN-SHOOT method, such as *e.g.* for what set of initial conditions (basin of attraction) is convergence guaranteed?, what is the rate of convergence within this basin? *etc.* Note, that these are all questions which can be answered (qualitatively at-least) in the context of the PSS-SHOOT algorithm employed herein. Use of the ngspice API is further complicated by its SPICE 3 heritage. From [17], this entails, among other things, that it is not possible to sort circuit elements based on their component class. This type of operation is, however, required in-order to implement the PNOISE module discussed above. Due to the circumstance described here, a decision was made to implement our own in-house PSS tool for the QUCS-COPEN project.

1.2 Outline of paper

Below, various theoretical and practical aspects *w.r.t.* the QUCS-COPEN PSS simulator engine are discussed. Sections 2, 2.1 and 2.2 reviews the theory behind the implemented algorithm whereas sections 2.3 and 2.4 discusses the various practical issues related to the actual implementation & integration of the tool into the QUCS-COPEN package. The text here will, in places, contain brief discussion of C++ code [21] (the QUCS program language) including the use of some C++ notation and keywords. In section 3, the new QUCS-COPEN PSS tool will be demonstrated on three example oscillator circuits. Examples are restricted to autonomous (clock) circuits as this aligns with the topic of this paper-series, *i.e.* (coupled)-oscillator phase-noise analysis. Then in section 3.1 the results produced by the developed PSS tool are validated through a comparison study w/ the commercial Keysight-ADS[®] EDA HB simulator. The section also contains a detailed discussion of the convergence properties of the implemented tool. Finally, section 4 summarizes the obtained results and outlines future work & projects, currently in the pipeline *w.r.t.* to the QUCS-COPEN project.

2 Background Theory & PSS Module Implementation.

The circuit equations are written using standard Modified-Nodal-Analysis (MNA) notation

$$\dot{q}(x(t)) + i(x(t)) + s(t) = 0 \quad (1)$$

where, $x(t) : \mathbb{R} \rightarrow \mathbb{R}^n$, represents the circuit state, assuming an n -dimensional system, with vectors, $q(x), i(x) : \mathbb{R}^n \rightarrow \mathbb{R}^n$, holding the reactive and resistive contributions, respectively, and $s(t) : \mathbb{R} \rightarrow \mathbb{R}^n$ representing the contributions of independent sources. Calculating the solution to eq. (1) represents an Initial-Value-Problem (IVP). The Linear-Response (LR) equations, generated from eq. (1), have the form

$$d(C(t)\delta x(t))/dt + G(t)\delta x(t) = 0 \quad (2)$$

where, $\delta x(t) : \mathbb{R} \rightarrow \mathbb{R}^n$, is the LR state vector, whereas, $C(t)=dq(s)/ds, G(t)=di(s)/ds|_{s=x(t)} : \mathbb{R} \rightarrow \mathbb{R}^{n \times n}$, are two time-dependent n -dimensional Jacobian matrices governing the LR system dynamics.

The PSS, $x_s(t) : \mathbb{R} \rightarrow \mathbb{R}^n$, represents a special solution of eq. (1), subject to the Boundary-Condition (BC)

$$x_s(t_0) = x_s(t_0 + T_0) \Leftrightarrow x_s(t_0) - x_s(t_0 + T_0) = 0 \quad (3)$$

with, $t_0 > 0$, being some offset and, $T_0 > 0$, the period of the PSS. Equation (1), subject to the eq. (3), then no longer constitutes an IVP but instead is classified as a (2-point) Boundary-Value-Problem (BVP). How to calculate the solution to such a BVP is not immediately obvious. It might seem possible to simply integrate eq. (1) until all transients have died out and then represent the PSS in-terms of this asymptotic solution. This brute-force approach is, however, entirely unworkable practice².

The QUCS-COPEN PSS calculator routine, documented herein, is designed around a kernel procedure modelled on the PSS-SHOOT algorithm, first described in [18, 22], and briefly reviewed below in section 2.2. Over the years, considerable research has gone into improving this time-domain methodology (see *e.g.* [19, 20, 23, 24, 27] for reviews) and the scheme has been employed in various important research and industrial projects (see *e.g.* Cadence SpectreRF[®] documentation). It represents a variant of the general *shooting-method* algorithm.

2.1 The Shooting-Method.

Consider the dynamical system in eq. (1) on the interval $t \in [t_a, t_b]$ subject to some unspecified BC. The solution procedure involves meshing interval into K sub-intervals $t_a = t_1 < t_2 < \dots < t_{K+1} = t_b$, and then defining [27]

$$G^q(x(t_i; s_{i-1}), s_j) = 0, \quad i = 1, 2, \dots, K+1, \quad j, q = 1, 2, \dots, K \quad (4)$$

where $G^q : \mathbb{R}^n \times \mathbb{R}^n \rightarrow \mathbb{R}^n$ is a series of K maps enforcing continuity at the mesh boundaries plus the BC at the endpoints, $x(t)$, is the state-vector (see eq. (1)) whereas, s_k , denotes the initial-value at mesh boundary t_k . For, $K > 1$,

²Electrical circuits generally represent stiff dynamical systems w/ widely separated time-constants which implies long transient integration time + small/narrow time-steps. Furthermore, the precision of a solution obtained using this approach would not suffice for subsequent sensitivity or noise-analysis.

the procedure is referred to as *multiple-shooting* [27] whereas, $K = 1$, describes the *single-shooting* scenario [18, 22]. Below, only single shooting is considered w/ the mesh $t_a = t_1 < t_2 = t_b$. At this point, a reduced notation is adopted in-order to keep expressions as simple as possible³. The solution at, $t_2 = t_b$, is then written, $x_\tau(x_0)$, with $\tau = t_b - t_a$ whereas, x_0 , represents the initial value at $t_1 = t_a$ (see footnote 3 for further explanation). Applying this new notation, the single-shooting variant of eq. (4) is written

$$F(x_0) = G^1(x_\tau(x_0), x_0) = 0 \quad (5)$$

The expression in eq. (5) transforms the original BVP into an IVP combined w/ the added problem of finding a root of an n -dimensional multivariate map. This is a well understood problem w/ several established solution procedures. Using *e.g.* a Newton-Raphson (NR) solver approach, w/ initial guess, $x_0^{(0)}$, (in the basin of attraction) a solution can be iterated as follows

$$x_0^{(l+1)} = x_0^{(l)} - [J^{(l)}]^{-1} F(x_0^{(l)}) \quad (6)$$

where, $x_0^{(l)}$, is the l th iterate of the solution, $F : \mathbb{R}^n \rightarrow \mathbb{R}^n$ is given in eq. (5), and $J^{(l)} \in \mathbb{R}^{n \times n}$ is the Jacobian of this map at $x_0^{(l)}$

$$J^{(l)} = \partial F(x_0^{(l)}) / \partial x_0^{(l)} = \Gamma_A^{(l)} \Phi_\tau^{(l)} + \Gamma_B^{(l)} \quad (7)$$

Here $\Gamma_A^{(l)}, \Gamma_B^{(l)} \in \mathbb{R}^{n \times n}$ are the l th iterate Jacobians of $G^1 : \mathbb{R}^n \times \mathbb{R}^n \rightarrow \mathbb{R}^n$ w.r.t. its arguments and, Φ_τ , is the sensitivity matrix

$$\Phi_\tau^{(l)} = \partial x_\tau(x_0^{(l)}) / \partial x_0^{(l)} \quad (8)$$

which can be calculated by integrating the LR equations in eq. (2) in parallel with the full solution, calculated through eq. (1).

2.2 The PSS-SHOOT Method.

The PSS-SHOOT method represents a special version the general algorithm discussed above. From section 2.1 and eq. (3), we consider the mesh $t_a = t_0$, $t_b = t_0 + T_0$ and $\tau = t_1 - t_0 = T_0$. From eq. (5), the PSS problem is then formulated

$$F_P(x_0) = G^1(x_T(x_0), x_0) = x_0 - x_T(x_0) = 0 \quad (9)$$

From eq. (6), in section 2.1, the root in eq. (9) is found through iteration

$$x_0^{(l+1)} = x_0^{(l)} - [J_P^{(l)}]^{-1} (x_0^{(l)} - x_T^{(l)}), \quad (10)$$

where the Jacobian, $J_P^{(l)}$, follows from eq. (7) subject to the PSS map in eq. (9). From inspection of eq. (9), $\Gamma_A = -I_n$ and $\Gamma_B = I_n$, (see discussion in section 2.1) where $I_n \in \mathbb{R}^{n \times n}$ is the n -dimnesional identity matrix. Inserting into eq. (7) gives

$$J_P^{(l)} = I - \Phi_T^{(l)} \quad (11)$$

with, $\Phi_T^{(l)} = \partial x_T(x_0^{(l)}) / \partial x_0^{(l)}$, being the l th iterated sensitivity matrix (see eq. (8) above).

³The initial value at $t_1 = t_a$ is represented by the symbol x_0 *i.e.* $s_1 \equiv x_0$ and thus $x(t_2; s_1) \equiv x(t_2; x_0)$. Given the interval, $\tau = t_b - t_a$, the solution at $t_2 = t_b$ is written $x(t_2; x_0) \equiv x_\tau(t_1, x_0)$. Finally, the absolute time-variable, t_1 , is eliminated from the expression, which leaves $x_\tau(x_0)$. Note, this expression implicitly contains the absolute time-variable index, t_1 , through the inclusion of x_0 which, by definition, is tied to this time-point. Hence, although not explicitly stated, the expression, $x_\tau(x_0)$, includes absolute time-dependence and thus represents a valid notation for both autonomous and non-autonomous systems.

2.2.1 The Autonomous Case.

The text above assumes that the frequency of operation, $f_0 = 1/T_0$, is a known fixed parameter. For autonomous circuits, *e.g.* free-running oscillators, this is of-course not the case. Below, the augmented PSS representation & operators, for the autonomous case, will be derived. In-order to limit notational complexity, the iteration index, $l \in \mathbb{Z}_{\geq 0}$, (see *e.g.* eq. (10)) will be neglected. From the discussion in sections 2.1 and 2.2 above, it should be clear how to re-introduce this index into the derived expressions.

The period, T_0 , is now a system variable and thus must be included in the state-vector. The augmented PSS state-vector, $\tilde{x}_0 : \mathbb{R}^{n+1}$ is then written

$$\tilde{x}_0 = [x_0 \quad T_0]^\top \quad (12)$$

With $n+1$ variables, the n -dimensional map in eq. (9) is now under-determined. To fix this issue, an additional equation, $\alpha^\top x_0 = 0$, is added to the system. Here, $\alpha \in \mathbb{R}^n$ is a constant n -dimensional vector and the introduced equation hence simply fixes of the phase of the PSS solution. The augmented PSS map is then written

$$\tilde{F}_P(\tilde{x}_0) = [F_P(\tilde{x}_0) \quad \alpha^\top x_0]^\top \quad (13)$$

where, F_P , is the map introduced above in eq. (9). The augmented Jacobian, defined as the derivative of the map in eq. (13), is then written from inspection

$$\tilde{J}_P = \begin{bmatrix} J_P & \Psi_T \\ \alpha^\top & 0 \end{bmatrix} = \begin{bmatrix} I - \Phi_T & \Psi_T \\ \alpha^\top & 0 \end{bmatrix} \quad (14)$$

where, J_P , is the original PSS Jacobian, Φ_T , is the sensitivity matrix (see eq. (11)) and the vector, $\Psi_T \in \mathbb{R}^n$, holds the components of vector, $-\partial x_T(x_0)/\partial T_0 \in \mathbb{R}^n$. Employing the augmented operators, eqs. (12) to (14), (w/ re-introduced iteration index (l)) in eq. (10) of section 2.2, the PSS-SHOOT algorithm is readily extended to include autonomous circuits.

2.3 Implementing the QUCS-COPEN PSS Module.

The QUCS-COPEN PSS module kernel is briefly outlined in algorithm. 1. As discussed above, this kernel is designed around the PSS-SHOOT algorithm reviewed above in sections 2.2 and 2.2.1. The module code resides within the new `pssolver` C++ class, which, in-turn, inherits directly from the existing `trsolver` class containing the `qucsator` transient engine implementation. For reasons discussed below, it was necessary to refactor and slightly rewrite, the original transient engine code in `trsolver`. Care was taken to maintain integrity of the original `qucsator` API, inline with our goal of extending the simulator w/o changing or destroying the interface and/or already existing functionality.

In algorithm. 1 (algorithm. 1) calls are made to transient engine subroutines `TranInit` and `TranPss`, both which are member methods belonging to the `trsolver` base-class. Here, calls of the type `Tran[Init/Pss](t_a, t_b, x_0)` both generate paths, $x(t_a) \rightarrow x(t_b)$, by integrating the IVP in eq. (1), subject to initial condition $x(t_a) = x_0$. Despite this similarity, the implementation of these two methods is notably different in-terms of *e.g.* initialization of solution state arrays, class state variable histories, the unwieldy large set of `trsolver` protected class members (acting as quasi-global state variables), various solver mode variables & switches, as well the invocation of allocation and clean-up/exit routines *etc.* The original `qucsator` API was simply not written to handle this level of flexibility described here *w.r.t.* different flavors of transient engine solver calls. This problem, in addition to a myriad of other implementation issues *w.r.t.* the `trsolver`->`pssolver` C++ inheritance architecture, triggered the refactoring of the QUCS-COPEN transient engine mentioned above.

The method, `collectGC`, called on algorithm. 1 of algorithm. 1 is a `pssolver` subroutine responsible for collecting the Jacobian matrices, $C(t)$, $G(t)$, introduced in eq. (2), along the path, $x_s(t)$, $t \in [t_0; t_0 + T_0]$ (see discussion *w.r.t.* `TranPss` above). This job is complicated somewhat by the fact that the `qucsator` implementation of the circuit equations does not employ the standard MNA format shown in eqs. (1) and (2). The `qucsator` circuit equations (transient analysis) are instead written [1] $A(t)x(t) = I_{eq}(t) + s(t)$, where, $A(t) : \mathbb{R} \rightarrow \mathbb{R}^{n \times n}$ represents the Jacobian matrix and $x(t)$, $s(t)$ again denote the system state/source-vectors (see eq. (1)). The vector function, $I_{eq}(t) : \mathbb{R} \rightarrow \mathbb{R}^n$, holds the *equivalent source vector* which contains past Linear-Multistep (LMS) terms of reactive components, nonlinear resistive component contributions and artificial offset terms which are included to fix double counting issues [1]. The two MNA representation discussed here (eq. (1) + the above) are obviously equivalent as they must produce the same set of KCL/KVL equations. From standard LMS theory, $A(t) = a_0 C(t) + G(t)$, where the scalar, $a_0 \in \mathbb{R}$,

Algorithm 1 QUCS-COPEN PSS Module Kernel.

Parameters : Tper, Tstab, MaxItr, EpsMax ▷ Tper : init. period guess, Tstab : stabilization time.
Input : x_{DC} ▷ calculated DC solution.
Output Datasets : init. tran. (Xt), PSS (Xp), abs. spec. (Xpa) ▷ DS file ext. w/ X=[V/I], Volt./Current.
Require: Tper > 0, Tstab ≥ 10 × Tper, MaxItr ≥ 10, EpsMax ≤ 10⁻⁶
Ensure: isNum(x_{DC}) = true ▷ check : x_{DC} is valid DC solution.

- 1: $x_{init} \leftarrow \text{TranInit}(0, Tstab; x_{DC})$
- 2: $t_0 \leftarrow Tstab, T_0 \leftarrow Tper$
- 3: $x_0^{(0)} \leftarrow x_{init}$
- 4: $x_T^{(0)} \leftarrow \text{TranPss}(t_0, t_0 + T_0; x_0^{(0)})$ ▷ eval PSS, $x_s^{(l=0)}(t) : x_s^{(l)}(t_0) = x_0^{(l)}, x_s^{(l)}(t_0 + T_0) = x_T^{(l)}$
- 5: $l \leftarrow 0, \text{done} \leftarrow \text{false}$
- 6: **while** done = false **and** $l \leq \text{MaxItr}$ **do**
- 7: $G^{(l)}(t), C^{(l)}(t) \leftarrow \text{collectGC}(x_s^{(l)}(t))$ ▷ eval $G^{(l)}(t), C^{(l)}(t)$ along path $x_s^{(l)}(t)$ (see eq. (2)).
- 8: $\Phi_T^{(l)} \leftarrow \text{Tran}\Phi(t_0, t_0 + T_0; x_0^{(l)})$ ▷ calc. sensitivity matrix (see eqs. (8) and (11)).
- 9: $J_P^{(l)} \leftarrow I - \Phi_T^{(l)}$
- 10: $F_P^{(l)} \leftarrow x_0^{(l)} - x_T^{(l)}$
- 11: $x_0^{(l+1)} \leftarrow x_0^{(l)} - [J_P^{(l)}]^{-1} F_P^{(l)}$
- 12: $x_T^{(l+1)} \leftarrow \text{TranPss}(t_0, t_0 + T_0; x_0^{(l+1)})$ ▷ generates $l+1$ th iterated PSS, $x_s^{(l+1)}(t)$, (see algorithm. 1
comment)
- 13: $\epsilon^{(l)} \leftarrow \|x_T^{(l+1)} - x_0^{(l+1)}\|$
- 14: **if** $\epsilon^{(l)} < \text{EpsMax}$ **then**
- 15: done ← true ▷ PSS solution found, exit routine,
- 16: **else**
- 17: $l \leftarrow l + 1$
- 18: **end if**
- 19: **end while**
- 20: $x_s(t) \leftarrow x_s^{(l+1)}(t)$ ▷ store iterated PSS solution.

depends on the specific LMS method and order employed. The matrix, $G(t)$, represents the DC Jacobian matrix function which can be calculated using the existing qucsator API. Subtracting this matrix from the above expression for the Jacobian allows for the evaluation of $a_0 C(t)$, and hence $C(t)$. The call to pssolver method, Tran Φ , on algorithm. 1 of algorithm. 1 then proceeds to calculate the circuit sensitivity matrix by integrating the LR equation in eq. (2) along the path, $x_s(t)$, using the matrix functions evaluated in collectGC. This LR method must follow the exact same LMS method & order, time-step mesh, program state histories *etc.* as the trsolver integration routine, TranPss, which generated $x_s(t)$.

2.4 The GUI Environment & Output Datasets.

As mentioned in section 1, the choice was made to link QUCS-COPEN extended simulator engine to QUCS-S GUI environment. Figure 1 illustrates newly implemented PSS tool operating inside this application. The figure shows the result of running a PSS simulation for some unspecified oscillator circuit. The PSS simulator (currently) outputs 3 datasets (see also algorithm. 1) : the stabilization transient (file-extensions .Vt, .It), the PSS time-domain solution (file-extensions .Vp, .Ip) and the PSS absolute-value spectrum (file-extensions .Vpa, .Ipa). From the figure it is also seen that the PSS analysis module has two main parameters : Tper & Tstab, which are described in the comments of algorithm. 1 (parameter section).

3 Example Oscillator Circuits.

Below, the QUCS-COPEN PSS solver is applied to three different oscillator circuits. As far as the authors can tell, the tool demonstrated here represents the first successful implementation of such a module, applicable to simulation of nonlinear autonomous circuits, into the QUCS ecosystem.

The first example considered is a simple Van-der-Pol equivalent circuit, shown fig. 2. The oscillator negative conductance is implemented using a QUCS Equation-Defined-Device (EDD) [2] w/ the current/voltage characteristic $I_n = a_0 + a_1 V + a_2 V^2 + a_3 V^3$, where $a_0 = a_2 = 0$ and $a_1 = -1.0\text{mS}$, $a_3 = 100.0\mu\text{A/V}^3$. Main PSS pa-

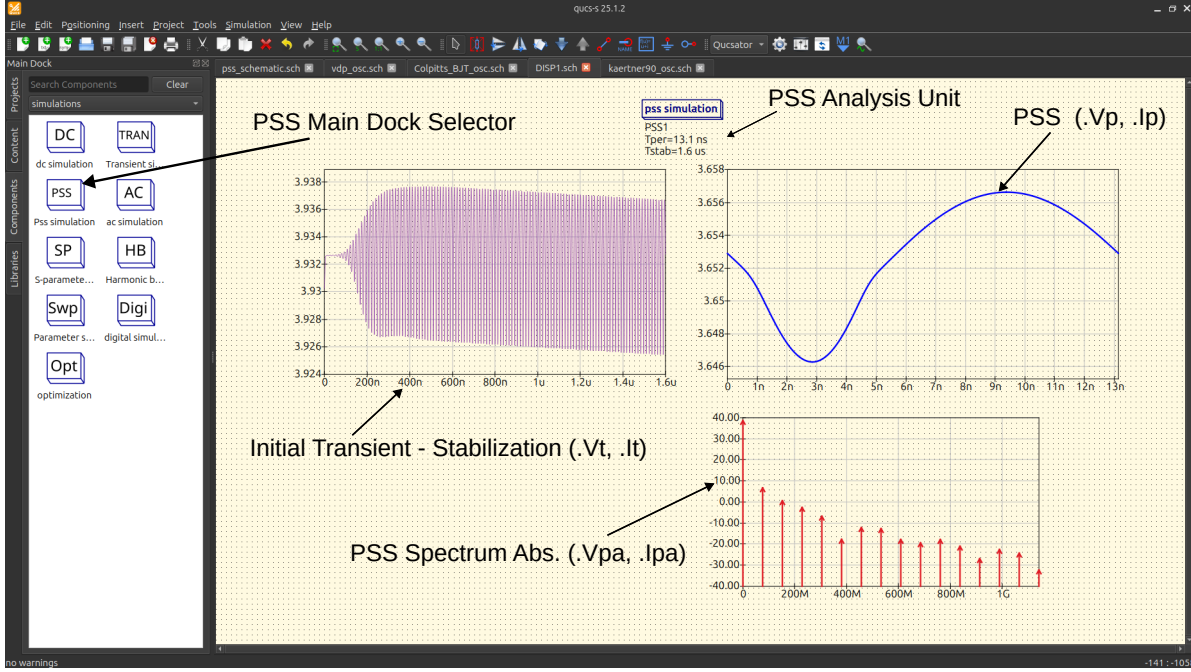


Figure 1: The figure shows the QUCS-COPEN PSS simulation unit integrated into the QUCS-S GUI environment. The analysis module is chosen from the main-dock and then placed on the schematic. The unit has two main parameters : Tper and Tstab, and the PSS precision is fixed in all experiments at $\text{EpsMax}=10^{-12}$ (see algorithm. 1) The 3 plotted graphs represent the 3 types of output datasets generated by the PSS simulator (unspecified oscillator circuit & output node). These are (w/ file extensions), **purple graph** : initial/stabilization transient, (.Vt, .It), **blue graph** : PSS time-domain solution, (.Vp, .Ip) and **red graph** : PSS solution, frequency-domain spectrum, absolute value, (.Vpa, .Ipa), which is plotted in dBm

rameters are set as : Tper = 1.0ns and Tstab = 30.5ns. The PSS module calculates a solution with oscillation frequency $f_0 = 1/T_0 = 896.6\text{MHz}$. The figure plots the PSS solution and abs. PSS spectrum datasets, see also section 2.4 and fig. 1 for details on datasets.

Figure 3 shows the same simulation setup as in fig. 2 but this time for a BJT Collpitts oscillator first proposed in the paper [25]. Compared with the original oscillator design, the circuit in fig. 3 includes a few modifications. Firstly, the resistor in the series LCR resonator was changed from 0.65Ohm in [25] to 1.65Ohm in the schematic shown here. Secondly, due to some internal qucsator BJT modelling issues (see footnote 4), which will be fixed in future releases of QUCS-COPEN, it was found necessary to neglect the BJT nonlinear base-resistance contribution⁴. Here, this internal component was cancelled by setting BJT model parameters Rbm = Rb = 0.0Ohm. All remaining contributions of the nonlinear BJT model are included in the simulation. The QUCS-COPEN PSS calculator finds a solution oscillating at, $f_0 = 76.07\text{MHz}$, and the output datasets are plotted for the external emitter node of the BJT device. Finally, fig. 4 shows the PSS module applied to a MOSFET cross-coupled pair, LC tank oscillator. The circuit is similar to the MOSFET oscillator proposed in [26, fig. 3] including identical device models. The circuit in fig. 4 differs from the original by the addition of inductor series resistances $r_s = 10.0\text{Ohm}$. The simulator finds a solution oscillating at, $f_0 = 888.6\text{MHz}$, and the PSS output datasets are plotted.

3.1 Verification of the Obtained PSS Solutions & Convergence Tests.

Define the measure, $\Gamma_f = (f_0^{\text{QC}} - f_0^{\text{K-ADS}})/f_0^{\text{QC}}$, where f_0^{QC} and $f_0^{\text{K-ADS}}$ are the steady-state oscillator frequencies calculated using the QUCS-COPEN PSS tool and the commercial Keysight-ADS[®] HB simulator, respectively. Thus, Γ_f

⁴After a rather lengthy debug session it was found that the qucsator code did not fully implement the Jacobian matrix contributions for the BJT base resistance. It only included the first-order contributions, *i.e.* the resistor itself, but not derivatives of the nonlinear characteristic. This type of modelling seems to suffice for DC, transient simulation *etc.*, however, the PSS calculation involves integrating the Jacobian (see section 2.3 and algorithm. 1), alongside the actual solution, and this modelling issue was found to lead to numerical instability problems.

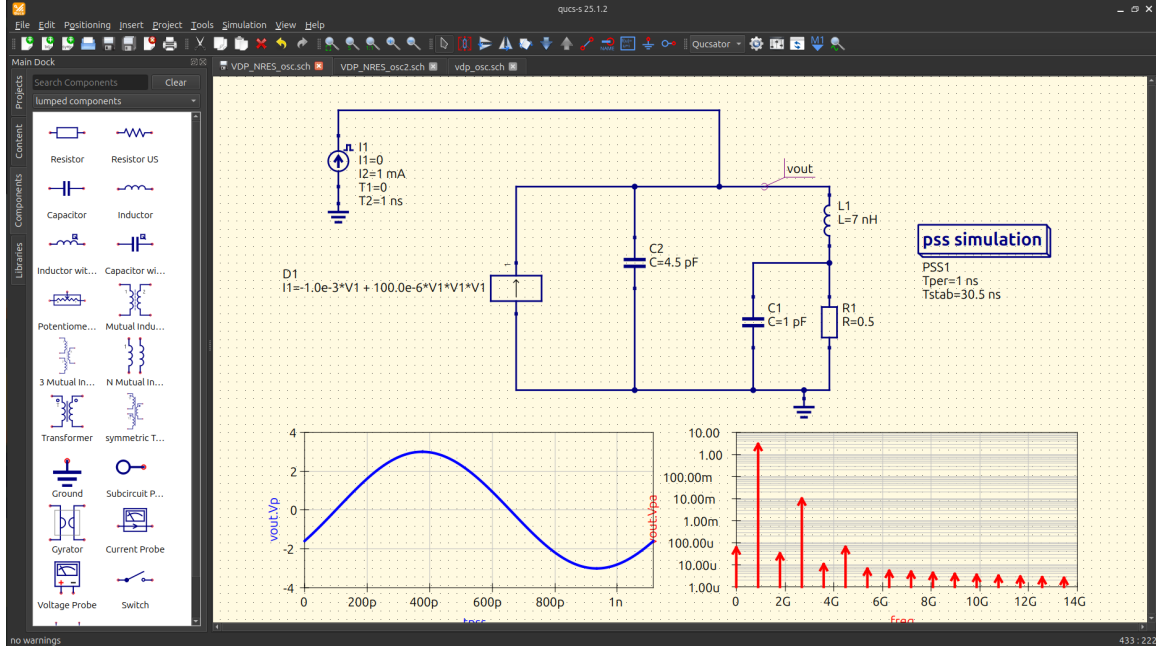


Figure 2: The figure shows the QUCS-COPEN PSS calculator applied to a simple Van-der-Pol(VDP)-type oscillator first proposed in [11, Fig. 3]. This circuit is referred to below as OSC. #1. All parameters are as in [11] (primary osc. parameter set). Two of the three available PSS datasets are plotted for the voltage node, vout, (stabilization transient data is not shown). Refer to fig. 1 caption for details.

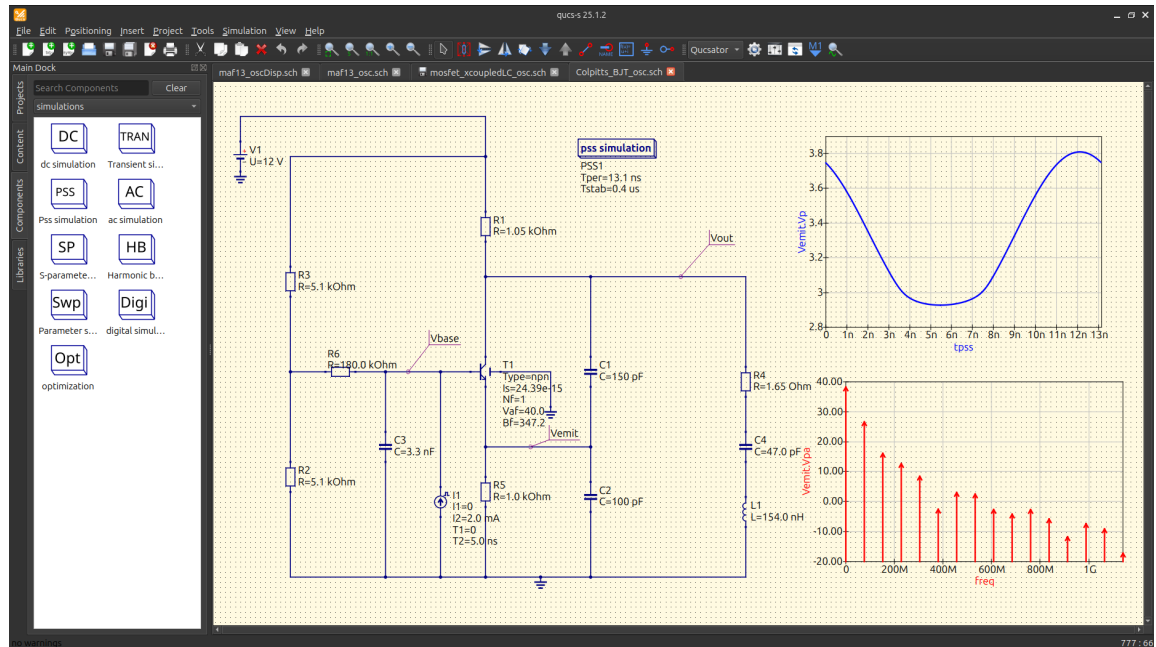


Figure 3: The simulator is applied to a BJT Colpitts oscillator taken from [25]. All circuit parameters as in [25], w/ the following exceptions : resonator resistor $r_0 = 1.65\text{Ohm}$ (was 0.65Ohm in the paper) and the BJT nonlinear base resistor is set to zero due to an internal qucsator BJT model issue (see footnote 4). This circuit is referred to below as OSC. #2. The figures plot the PSS output datasets for the external BJT emitter node, referred to as, Vemit, in the schematic. See the captions of figs. 1 and 2 for details.

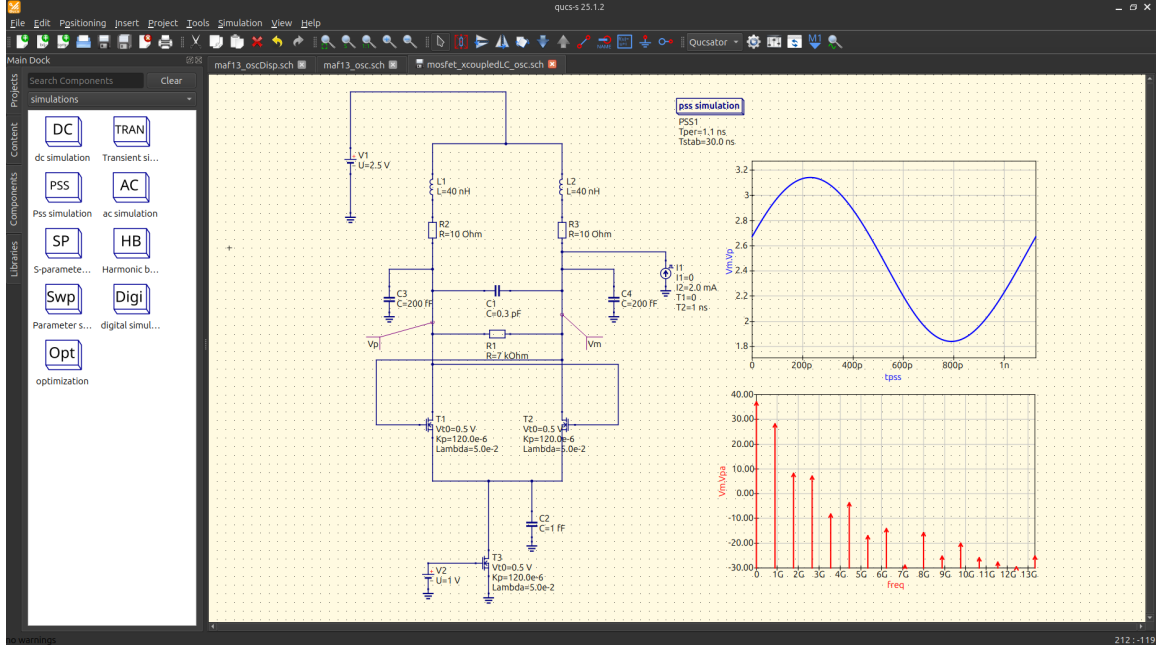


Figure 4: Figure shows the QUCS-COPEN PSS simulation tool applied to a MOSFET cross-coupled LC-tank oscillator. The circuit is similar to the oscillator proposed in [26, fig. 3] with minor variations (see text). This circuit is referred to below as OSC. #3. The figures plot the PSS output datasets for the right-hand MOSFET device drain-node, referred to as, V_m , in the schematic. See also figs. 1 and 2 for details.

	QUCS-COPEN	Keysight-ADS [®]	$ \Gamma_f $
OSC. #1	896.62903MHz	896.64032MHz	0.00126%
OSC. #2	76.069172MHz	76.075090MHz	0.00778%
OSC. #3	888.58810MHz	888.59892MHz	0.00122%

Table 1: The table lists PSS oscillator frequencies calculated using the QUCS-COPEN package and the commercial Keysight-ADS[®] simulator for circuits : OSC. #1 = VDP circuit in fig. 2, OSC. #2 = BJT circuit in fig. 3 and OSC. #3 = MOSFET circuit in fig. 4. The relative deviation between the calculated values are recorded by measure Γ_f (see text in section 3.1).

records, for a given oscillator circuit, the deviation of PSS frequencies calculated applying these two very different EDA programs. Table 1 displays the calculated PSS frequencies and the resulting measure, $|\Gamma_f|$, for each of the three oscillators discussed above in section 3. The maximum measured relative error is $|\Gamma_f| \sim 0.008\%$, or $|\Gamma_f| \sim 80\text{ppm}$ (parts-per-million). The results listed in table 1 serve to validate the developed QUCS-COPEN PSS tool.

Two PSS convergence measures are defined

$$\epsilon(l) = \|x_s^{(l)} - \bar{x}_s\| \quad (15)$$

$$\Delta f(l) = \|f_0^{(l)} - \bar{f}_0\| / \bar{f}_0 \quad (16)$$

where $\epsilon(l) : \mathbb{Z}_{\geq 0} \rightarrow \mathbb{R}$, in eq. (15), represents the precision of the l th iterated PSS solution, $x_s^{(l)}$, (see sections 2.2 and 2.3 and algorithm. 1) with \bar{x}_s denoting the true PSS solution; *i.e.* the numerically calculated PSS solution. Likewise, $\Delta f(l) : \mathbb{Z}_{\geq 0} \rightarrow \mathbb{R}$, in eq. (16), measures the relative frequency precision of the l th iterated solution with $f_0^{(l)}$ and \bar{f}_0 denoting the frequency of the l th iterate and the true PSS frequency (*i.e.* frequency of \bar{x}_s), respectively. To quantify initial conditions of experiments below, two further measures are defined

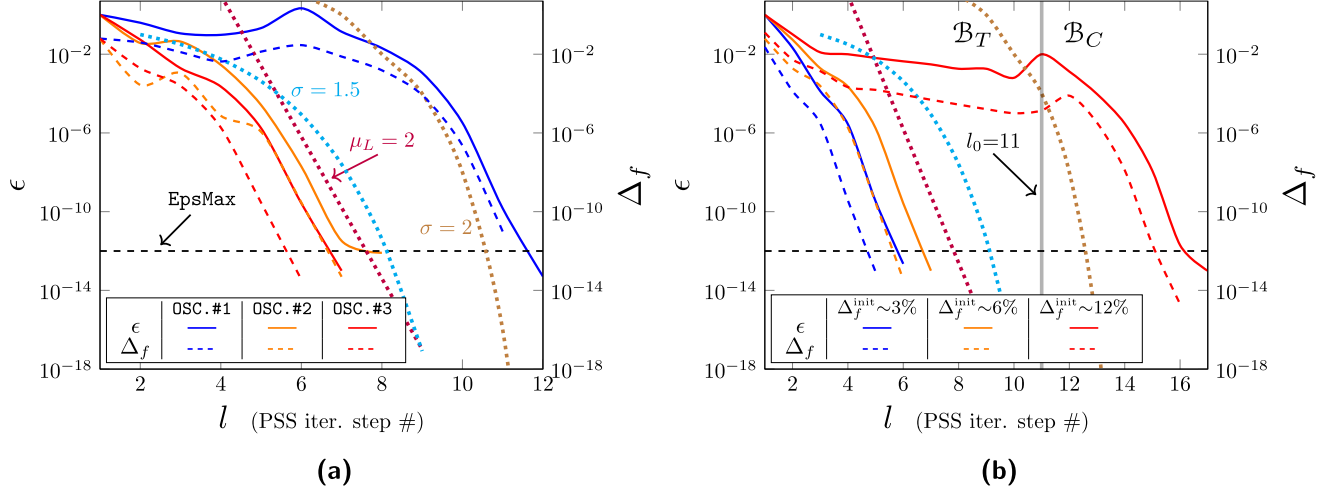


Figure 5: Convergence measures, ϵ (solid line left y-axis), and Δ_f (dashed line, right y-axis), defined in eqs. (15) and (16), plotted as a function of the PSS iteration index l (see sections 2.1 and 2.2 and algorithm. 1) for different circuits and parameter configurations. Dotted curves represent sequences of varying convergence order σ (see section A) : $\sigma = 2$ (brown $\cdot \cdot \cdot$), $\sigma = 1.5$ (cyan $\cdot \cdot \cdot$), $\sigma = 1$ (purple $\cdot \cdot \cdot$) w/ linear convergence rate $\mu_L = 2$. (a) : PSS measures, ϵ , Δ_f , are plotted for each of the oscillators OSC.#1-3 (see table 1 caption & figs. 2 to 4) w/ initial conditions, $\Delta_f^{\text{init}} \sim 6\%$ and $K_{\text{STAB}} \sim 30-35$ (see eqs. (17) and (18)). (b) : figure plots the PSS measures for circuit OSC.#3, for 3 different initial conditions as specified by the parameter Δ_f^{init} and w/ $K_{\text{STAB}} \sim 30-35$.

$$\Delta_f^{\text{init}} := \Delta f(0) \quad (17)$$

$$K_{\text{STAB}} := \text{Tstab} \bmod \bar{T}_0 \quad (18)$$

where Δ_f^{init} is the relative error of the initial PSS frequency guess and K_{STAB} represents the stabilization interval (see algorithm. 1) expressed to the nearest multiple of the PSS period $\bar{T}_0 = 1/\bar{f}_0$.

Figure 5 shows the results of a series of convergence experiments expressed in-terms of the measures defined above in eqs. (15) and (16). Specifically, fig. 5.(a) plots these two measures as a function of the iteration index, $l \in \mathbb{Z}_{\geq 0}$, for each of the three oscillator circuits, OSC.#1-3, shown in figs. 2 to 4, for a fixed set of initial conditions ($\Delta_f^{\text{init}}, K_{\text{STAB}}$) whereas fig. 5.(b) plots the measures for the OSC.#3 circuit (see fig. 4), for a range of initial conditions, as described by Δ_f^{init} in eq. (17).

3.1.1 The Convergence Zone \mathcal{B}_C .

Initial conditions, leading to convergence are said to lie inside the solver's *basin of attraction*. Inspecting fig. 5 this basin can be divided (roughly) into two main regions : the initial transition zone/region, \mathcal{B}_T , where the solver does not really converge but traverses the state-space until a suitable point is reached. Once this happens the solver enters the convergence zone/region, \mathcal{B}_C . Denote the iteration step where the solver state enters \mathcal{B}_C , or leaves \mathcal{B}_T , as $l_0 \in \mathbb{Z}_{\geq 0}$. The markers $\mathcal{B}_T, \mathcal{B}_C, l_0$ are illustrated in fig. 5.(b), for $\Delta_f^{\text{init}} \sim 12\%$ (red curves), where the solver is seen to enter the convergence zone around $l = l_0 = 11$. Obviously, the goal is to enter \mathcal{B}_C as quickly as possible, or equivalently, minimize the number of steps inside \mathcal{B}_T . Generally, l_0 should decrease w/ Δ_f^{init} , as this will move the solver initial state towards a perfect PSS frequency guess (see eqs. (15) and (17)). Thus, we expect to observe, $l_0 \rightarrow 0$, for, $\Delta_f^{\text{init}} \rightarrow 0$. Inspecting fig. 5.(b), this trend can indeed be observed, *i.e.* improving the frequency guess leads to quicker PSS convergence. Empirical rules, of the type discussed above, however only describe a trend and do not guarantee that the relation always hold. Figure 5.(a) illustrates this issue as circuits OSC.#2-3 display as much smaller l_0 (reaches \mathcal{B}_C faster) compared to OSC.#1 for identical initial conditions. It should be possible to advance the robustness of the QUCS-COPEN PSS algorithm by introducing *e.g.* multiple-shooting solver methods [27] (see also section 2.1) and implementing global & local solver dampening techniques [24]. It will furthermore be interesting to look into employing Krylov (matrix-free) linear solvers [19, 20], something not currently available in the QUCS package, which

should significantly increase efficiency, especially for large circuits. The ideas mentioned above will all be considered for future work on the QUCS-COPEN project.

3.1.2 The Convergence Rate Inside \mathcal{B}_C .

We seek to quantify the convergence order & rate for the QUCS-COPEN PSS module experiments in fig. 5 inside convergence zone \mathcal{B}_C . The basic concepts required for this discussion are reviewed in section A. For our purposes, 3 additional sequences, w/ 3 convergence orders are plotted in fig. 5 (dotted curves, see caption for details). Comparing the convergence curves w/ these added test-sequences, the following observations *w.r.t* the rate of convergence inside \mathcal{B}_C can be stated.

1. the solver never obtains the ideal Newton solver quadratic convergence ($\sigma = 2$).
2. the convergence order inside, \mathcal{B}_C , is larger than 1, *i.e.* faster than linear-convergence.
3. from inspection of the various curves in fig. 5, a rough estimate of the convergence order inside, \mathcal{B}_C , could be around $\sigma = 1.5$ (compare with brown dotted curve).
4. the linear-convergence test-sequence (purple dotted) represents a rough tangential to the convergence curves around the PSS convergence point, $\epsilon_c = \text{EpsMax}$. Hence, in a small region around ϵ_c the error sequence measures, $\epsilon(l)$, $\Delta_f(l)$, defined in eqs. (15) and (16), can be approximated as linear sequences w/ convergence rate $\mu_L = 2$.

Let, σ_{QC} , denote the convergence order of the QUCS-COPEN PSS module, it then follows from the remarks that, $\sigma_{QC} \sim 1.5$, inside \mathcal{B}_C . Furthermore, from item 4 in the above list, since the linear approximation close to convergence, $\epsilon \simeq \epsilon_c$, has convergence-rate $\mu_L = 2$, it follows that the precision of the solution, as measured by the closeness of, ϵ , Δ_f , to zero, increases two decimal digits for each iteration step in this area (see section A for details).

The QUCS-COPEN PSS module is not able to attain the ideal Newton-solver quadratic convergence. However, this should not be too surprising. This quadratic convergence rule, often quoted, is an idealized theoretical result and does not take into account the various issues involved with implementing a real-world numerical PSS solver, such as *e.g.* operating w/ finite number precision, non-ideal linear matrix solvers, considering a nonlinear map which, implicitly, involves a IVP which brings a whole new set of issues (*e.g.* truncation error, internal linear solver errors) *etc.* This is however not to say that there is no room for improvement, as this is almost certainly the case. We intend to explore various schemes for advancing the PSS tool *w.r.t.* convergence rate, including, implementing the ideas discussed above in section 3.1.1.

4 Conclusion & Future Work.

The paper documents the work done implementing a periodic steady-state analysis module, based around a single-shooting/Newton-solver kernel algorithm, into the novel QUCS-COPEN simulator engine; a clone the QUCS and QUCS-S software projects. The work advances the state of the QUCS project as this represents, to our knowledge, the first time such a tool, applicable to autonomous circuits, has been developed for this environment. The PSS module was validated through a comparison-study w/ the commercial Keysight-ADS[®] EDA program and the convergence properties were analyzed w/ proposals and ideas for improving robustness and efficiency of the algorithm. Future work will focus on increasing the reliability & efficiency of the tool by exploring more robust multiple-shooting solvers and using more elaborate solver dampening schemes to ensure convergence even for weak initial conditions. We furthermore intend to investigate the possible use of Krylov (matrix-free) linear-solvers which should increase the performance of the engine significantly, especially for larger circuits. The long-term goal of the work, described herein, is the development of a novel (coupled)-oscillator phase-noise analysis module to be integrated into the QUCS-COPEN distribution. This module builds on top of the steady-state tool described herein, and it is the topic of the second part of this paper-series.

Acknowledgment

The authors gratefully acknowledge partial financial support by German Research Foundation (DFG) (grant no. KR1016/17-1).

A Brief Summary of Convergence Order & Rate.

An iterated sequence, f_k , which converges asymptotically towards zero, $\lim_{k \rightarrow \infty} f_k = 0$, is said to have asymptotic convergence order & rate, σ, μ , if $\lim_{k \rightarrow \infty} |f_{k+1}|/|f_k|^\sigma = \mu$. Here $\sigma = 1$ is called linear-convergence whereas $\sigma = 2$ refers to quadratic-convergence and so on. Note that, $\sigma = 1$, is referred to as "linear" convergence since a sequence, plotted w/ a log-linear axis configuration, will produce a straight line. Hence, "linear" convergence, in this context, actually implies exponential convergence curve whereas, $\sigma > 1$, denotes convergence faster than exponential. The Newton-Raphson (NR) solver, upon which the PSS algorithm discussed herein is based on, is known to converge w/ at-least quadratic order, in small open region containing the root. For linear convergence order, $\sigma = 1$, it is usual practice to introduce the convergence rate as $\mu_L = -\log_{10}(\mu)$ which expresses the number of decimal digits the solution improves, per iteration step. Thus, let f_k be a sequence w/ linear convergence towards 0 and let $\mu_L = m$. In this case, the error, $e_k = |f_k|$, moves m decimal digits closer to zero for each iteration step.

References

- [1] S. Jahn, M. Margraf, V. Habchi, and R. Jacob. Qucs technical papers. Technical report, 2007.
- [2] S. Jahn and J. C. Borrás. Getting started with qucs. Technical report, March 2007.
- [3] Mike Brinson and Vadim Kuznetsov. Qucs equation-defined and verilog-a rf device models for harmonic balance circuit simulation. In *2015 22nd International Conference Mixed Design of Integrated Circuits & Systems (MIXDES)*, pages 192–197. IEEE, 2015.
- [4] Mike Brinson and Vadim Kuznetsov. Qucs-0.0. 19s: A new open-source circuit simulator and its application for hardware design. In *2016 International Siberian Conference on Control and Communications (SIBCON)*, pages 1–5. IEEE, 2016.
- [5] Mike Brinson and Vadim Kuznetsov. Improvements in qucs-s equation-defined modelling of semiconductor devices and ic's. In *2017 MIXDES-24th International Conference" Mixed Design of Integrated Circuits and Systems*, pages 137–142. IEEE, 2017.
- [6] Torsten Djurhuus, Viktor Krozer, J Vidkjar, and Tom K Johansen. Trade-off between phase-noise and signal quadrature in unilaterally coupled oscillators. In *IEEE MTT-S International Microwave Symposium Digest, 2005.*, pages 883–886. IEEE, 2005.
- [7] Torsten Djurhuus, Viktor Krozer, Jens Vidkjær, and Tom K Johansen. Nonlinear analysis of a cross-coupled quadrature harmonic oscillator. *IEEE Transactions on Circuits and Systems I: Regular Papers*, 52(11):2276–2285, 2005.
- [8] Torsten Djurhuus, Viktor Krozer, Jens Vidkjær, and Tom K Johansen. Am to pm noise conversion in a cross-coupled quadrature harmonic oscillator. *International Journal of RF and Microwave Computer-Aided Engineering: Co-sponsored by the Center for Advanced Manufacturing and Packaging of Microwave, Optical, and Digital Electronics (CAMPmode) at the University of Colorado at Boulder*, 16(1):34–41, 2006.
- [9] Torsten Djurhuus, Viktor Krozer, Jens Vidkjær, and Tom K Johansen. Oscillator phase noise: A geometrical approach. *IEEE Transactions on Circuits and Systems I: Regular Papers*, 56(7):1373–1382, 2008.
- [10] Torsten Djurhuus and Viktor Krozer. A study of amplitude-to-phase noise conversion in planar oscillators. *International journal of circuit theory and applications*, 49(1):1–17, 2021.
- [11] Torsten Djurhuus and Viktor Krozer. A generalized model of coupled oscillator phase-noise response. *International journal of circuit theory and applications*, 50(1):35–55, 2022.
- [12] GNU Project - the Free Software Foundation. *GnuCap Manual*, January 2024. Available at <http://www.gnucap.org/dokuwiki/doku.php/gnucap:manual:introduction>.
- [13] Paolo Nenzi Holger Vogt, Giles Atkinson. *Ngspice User's Manual Version 44plus*, June 2025. Available at <https://ngspice.sourceforge.io/docs/ngspice-manual.pdf>.
- [14] Eric R. Keiter. *Xyce™ Parallel Electronic Simulator User's Guide*. Sandia National Lab.(SNL-NM), Albuquerque, NM (United States), 2025. Available at <https://xyce.sandia.gov/documentation-tutorials/>.
- [15] Stefano Perticaroli, Paolo Nenzi, Fabrizio Palma, et al. A novel pss analysis implementation reusing the tran analysis of ngspice circuit simulator. In *Proceedings of 2011 MOS-AK Workshop*, 2011.
- [16] Francesco Lannutti and Stefano Perticaroli. Klu and pss analysis implementations into ngspice. MOS-AK 2012, December 2012.

- [17] Wlodek Grabinski, Mike Brinson, Paolo Nenzi, Francesco Lannutti, Nikolaos Makris, Angelos Antonopoulos, and Matthias Bucher. Open-source circuit simulation tools for rf compact semiconductor device modelling. *International Journal of Numerical Modelling: Electronic Networks, Devices and Fields*, 27(5-6):761–779, 2014.
- [18] TJJR Aprille and T Trick. A computer algorithm to determine the steady-state response of nonlinear oscillators. *IEEE Transactions on Circuit Theory*, 19(4):354–360, 1972.
- [19] Ricardo Telichevesky, Kenneth S Kundert, and Jacob K White. Efficient steady-state analysis based on matrix-free krylov-subspace methods. In *Proceedings of the 32nd annual ACM/IEEE Design Automation Conference*, pages 480–484, 1995.
- [20] Kundert. Simulation methods for rf integrated circuits. In *1997 Proceedings of IEEE International Conference on Computer Aided Design (ICCAD)*, pages 752–765. IEEE, 1997.
- [21] Bjarne Stroustrup. *The C++ programming language*. Pearson Education, 2013.
- [22] Thomas J Aprille and Timothy N Trick. Steady-state analysis of nonlinear circuits with periodic inputs. *Proceedings of the IEEE*, 60(1):108–114, 1972.
- [23] Kai Bittner and Hans Georg Brachtendorf. Multirate shooting method with frequency sweep for circuit simulation. In *Scientific Computing in Electrical Engineering: SCEE 2016, St. Wolfgang, Austria, October 2016*, pages 113–125. Springer, 2018.
- [24] Makiko Kakizaki and Tsutomu Sugawara. A modified newton method for the steady-state analysis. *IEEE transactions on computer-aided design of integrated circuits and systems*, 4(4):662–667, 1985.
- [25] Franz X Kaertner. Analysis of white and f- α noise in oscillators. *International Journal of Circuit Theory and Applications*, 18(5):485–519, 1990.
- [26] Paolo Maffezzoni, Federico Pepe, and Andrea Bonfanti. A unified method for the analysis of phase and amplitude noise in electrical oscillators. *IEEE transactions on microwave theory and techniques*, 61(9):3277–3284, 2013.
- [27] Jeffrey R Parkhurst and Lawrence L Ogborn. Determining the steady-state output of nonlinear oscillatory circuits using multiple shooting. *IEEE transactions on computer-aided design of integrated circuits and systems*, 14(7):882–889, 2002.